

A Vehicle Flow Counting System in Rainy Environment Based on Vehicle Feature Analysis

Deng-Yuan Huang¹, Chao-Ho Chen^{2,*}, Tsong-Yi Chen², Wu-Chih Hu³, Yu-Lin Lin²

¹Department of Electrical Engineering, Da-Yeh University
168, University Rd., Dacun, Changhua 51519, Taiwan, R.O.C.
kevin@mail.dyu.edu.tw

²Department of Electronic Engineering, National Kaohsiung University of Applied Sciences
415 Chien Kung Rd., Kaohsiung 807, Taiwan, R.O.C.
thouho@kuas.edu.tw

³Department of Computer Science and Information Engineering
National Penghu University of Science and Technology
300 Liu-Ho Rd., Makung, Penghu 880, Taiwan, R.O.C.
wchu@npu.edu.tw

*Corresponding author: Chao-Ho Chen

Received August, 2015; revised September, 2015

ABSTRACT. *A feature-based vehicle counting system is presented for a traffic surveillance system under rainy conditions. The proposed method integrates the subsystems of background subtraction, removals of shadows and headlights, raindrop filtering, vehicle tracking and classification to achieve robust traffic counting. In the background subtraction model, background pixels are determined based on the selection of the most occurrence of grayscale for each point. The spatial accuracy of the segmentation of moving objects is greatly improved by raindrop filtering in rainy conditions. Analysis of the features of aspect ratio, area ratio, and compactness of vehicles shows that the highest recognition rate of moving targets can be achieved using the feature of aspect ratio. The tracking of moving targets is conducted by comparing extracted features and by measuring the minimum distance of centroids of objects between consecutive images. To increase the accuracy of vehicle classification, the temporal correlation of moving objects in successive frames is taken into consideration. Experimental results show average counting accuracies of 88.1% and 84.9% for cars and bikes, respectively, on a city road, and 86.9% and 96.3% for the lanes of TOWARDS and AWAY, respectively, on a highway, indicating the feasibility of the proposed method for traffic counting.*

Keywords: Intelligent transportation system (ITS), Object segmentation, Background subtraction, Raindrop filtering, Vehicle feature.

1. **Introduction.** Intelligent transportation systems (ITSs) are often considered an effective method for solving the problems of traffic congestion. The performance of ITSs highly depends on the accuracy of the measure of traffic flow, which is usually measured in terms of vehicles per hour. Therefore, accurate vehicle counting is critical to real-time ITSs, which are expected to work well under all weather conditions. Taiwan is an island in the western North Pacific Ocean through which the Tropic of Cancer passes in the middle. The island has a monsoon climate, with wet summers and dry winters. The rainy season brings almost daily showers from May to June, and an average of 4 typhoons directly hit

the island from July to October. Therefore, it is important to consider the effect of rain on the performance of traffic surveillance systems in Taiwan.

Most methods for vehicle flow measurement perform well in fine weather, but they may fail to operate in rainy conditions. The present study proposes a vehicle counting system that operates well in rainy conditions and various types of road (city roads and highways). In the proposed method, image sequences are first captured by a color video camera set up at the roadside of city roads or highways. Then, raindrops are removed from the background if necessary. Raindrop filtering greatly increases the accuracy of moving-object segmentation due to the elimination of interference. Methods for dealing with shadows and vehicle headlights are also proposed. The major contribution of this paper is the integration of raindrop, shadow, and headlight removal, which greatly increases the reliability of vehicle counting.

Motion detection in many tracking systems involves background subtraction. Generally, there are two types of Gaussian method for background subtraction: single Gaussian [1] and a mixture of Gaussians [2]. Wren et al. [1] developed a real-time tracking system called Pfinder (person finder) that uses a multi-class statistical model for tracked objects, with the background being modeled as a single Gaussian for each pixel. This system can track a single moving person in indoor environments. However, the performance of this tracker for outdoor scenes has not been reported. The mixture of Gaussians is more suitable than a single Gaussian for dealing with slow lighting changes, slow-moving objects, and camera noise. Stauffer and Grimson [2] used a mixture of adaptive Gaussians to represent the color distribution of each pixel to handle variations such as lighting, shadows, and camera noise. By updating parameters, their system can track people and cars in outdoor environments.

Recently, Mandellos et al. [3] proposed a background subtraction method based on the histogram of the $L^*u^*v^*$ color space for constructing an on-demand background template to overcome the common weaknesses of initialization and background updating in existing background subtraction algorithms. Their background model can deal with unstable lighting, different view angles, and heavy congestion, making it capable of detecting vehicles in realistic traffic scenes. Zhang et al. [4] presented a high-order texture pattern flow (TPF), which is used to encode the variations of binary pattern among pixel neighborhoods in the space-time domain, for background modeling and moving-object detection. The combination of the Gaussian mixture model (GMM) and the integral histogram feature of TPF is then used to estimate an adaptive threshold for a histogram similarity measure to determine whether a pixel belongs to the background or a moving object.

To detect vehicles in traffic surveillance sequences, background initialization, foreground detection, and background updating are three essential procedures. Once objects are detected, object tracking is carried out, which can be usually classified as region-based tracking, active contour-based tracking, feature-based tracking, and model-based tracking. In region-based tracking [5], the variations of connected regions in images corresponding to moving objects are detected to achieve object tracking. Active contour-based tracking [6] uses object silhouettes as a bounding contour and updates the contour dynamically in successive frames. Feature-based tracking [7, 8, 9] uses features of objects, such as shape, area, color, corners, and vertices, and then matches these features between successive frames to achieve object tracking. In model-based tracking [10], object tracking is performed by matching a projected object model to image data, where the object model is produced with prior knowledge.

Feature-based tracking methods are the most widely used due to their robustness; even with partial occlusion, some of the features of moving objects are still visible, and the approach can adapt to varying illumination, such as daylight, twilight, or nighttime

conditions. In general, the features of a moving object can be classified as: (1) global feature-based, such as the center of gravity, color, and area [8]; (2) local feature-based, such as corners [9]; and (3) dependence graph-based [7], such as structure changes between graphs. However, since tracking performance highly depends on the selection of features, there is a problem of grouping, i.e., what set of features belongs to a moving object. In this paper, a more salient feature of vehicles is proposed for classifying vehicles into cars or bikes, where cars include buses and trucks, and bikes refer to two-wheel vehicles, such as bicycles, motorcycles and scooters.

Most video surveillance systems operate well in good weather conditions, which is the case for only half the year in Taiwan. The performance of existing methods may significantly degrade in rainy conditions. The effects of rain on a video surveillance system in a natural environment have seldom been explored. Garg and Nayar [11] developed a correlation model to analyze the visual effects of rain on imaging systems. Based on the model, they presented an efficient algorithm for detecting and removing raindrops from video sequences. They observed that raindrops have higher brightness than the corresponding background intensities in their experiments. Recently, DASs equipped with in-vehicle cameras that can remove the interference of raindrops have been developed [12, 13].

The rest of this paper is organized as follows. In Section 3, the proposed method for vehicle counting, which consists of background subtraction, the removal of shadow and headlight illumination, raindrop filtering, feature extraction, vehicle tracking, and classification schemes, is described. Section 4 presents the experimental results and a discussion. The conclusions are given in Section 5.

2. The proposed method. A flowchart of the proposed method for vehicle counting in rainy conditions is shown in Fig. 1. Moving objects are first segmented from a video sequence using motion detection and background updating schemes. Motion detection is used to analyze the temporal correlation of moving objects in successive frames. A frame difference mask and a background subtraction mask are utilized to acquire the initial object mask, using which the problem of stationary objects in backgrounds can be well solved. In rainy conditions, the removal of raindrops is then carried out. Boundary refinement is used to reduce the influence of shadows and solve the problem of residual background areas. Each segmented object, denoting a vehicle, is then bounded by a rectangle; the height, width, and area of the rectangle are regarded as important features of that vehicle. Based on the extracted features, each vehicle can be classified as being either a car or a bike.

Traffic cameras are often set up at roadsides. In such case, the scheme of background subtraction [1, 2, 3, 4] is suitable for detecting moving vehicles because the backgrounds in the video streams are stationary. In this paper, background modeling based on the temporal distribution of gray levels is built for each point, by which the gray level with maximum occurrence probability is assigned to that of the absolute background. As to the detailed information of how to build this model, the readers can refer to our previously published paper [14].

2.1. Removal of shadows and headlights. Moving objects cast shadows due to light fluctuation in outdoor situations, which is a common scenario in many applications for traffic surveillance systems. Shadows can lead to serious deformation of objects when moving objects are segmented from the background due to them being erroneously recognized as part of the foreground. Therefore, shadow detection is critical to accurately detecting moving objects. In this work, a shadow detection model is proposed that uses

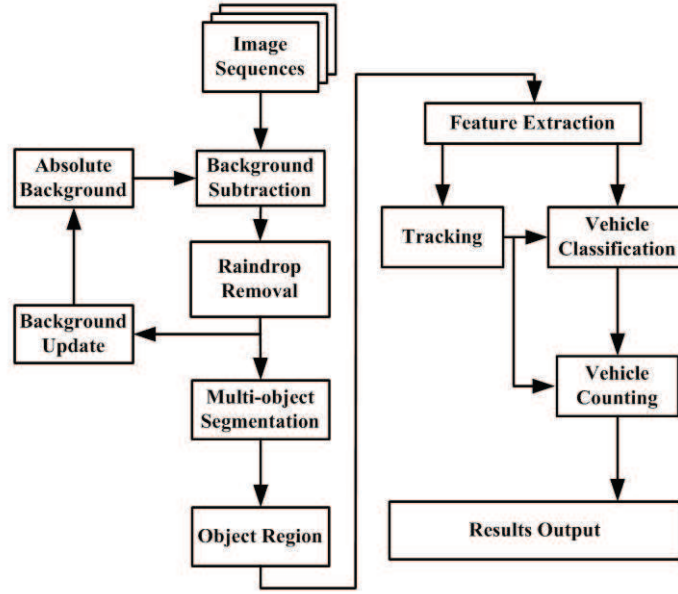


FIGURE 1. Flowchart of proposed method for vehicle counting in rainy conditions

spectral features based on the HSV color space; the method is motivated by the work of Cucchiara et al. [15] and Prati et al. [16]. The HSV color space is close to the human perception of colors and thus allows shadows to be accurately distinguished.

Let $I_t^V(p)$ and $B_t^V(p)$ be the light intensities of the current frame and its background, respectively, at the point $p(x, y)$ for the t th frame in a video sequence. The light intensity ratio, $\xi_t(p)$, can be defined as:

$$\xi_t(p) = I_t^V(p)/B_t^V(p) \quad (1)$$

where $\xi_t(p) > 1$ represents the points of moving objects that are brighter than those of the background; otherwise, $\xi_t(p) < 1$ for shadow points. Using the ratio of light intensity of the current frame to that of the background, the proposed shadow detection model is given as:

$$\lambda_t(p) = \begin{cases} 1, & \text{if } (\alpha_1 \leq \xi_t(p) \leq \alpha_2 \text{ and} \\ & |I_t^S(p) - B_t^S(p)| \leq \tau_s \text{ and} \\ & |I_t^H(p) - B_t^H(p)| \leq \tau_H) \\ 0, & \text{otherwise} \end{cases} \quad (2)$$

Shadow points are detected when $\lambda_t(p) = 1$; otherwise the points belong to moving objects. To allow some noise in the background image, the value of α_2 in this work is taken as 0.95. It was observed that when the value of $\xi_t(p)$ was too low, some shadow points were misclassified as belonging to moving objects; therefore, the value of α_1 is set to be 0.65 for our work. In general, α_1 can be viewed as the power of the shadow, i.e., the strength of the relation between the light source and the reflectance and irradiance of the objects. Thus, for strong sunshine, a lower α_1 is preferable [16] In Eq. (2), $I_t^S(p)$ and $B_t^S(p)$ represent the saturation values in the HSV color space for the t th frame and its background, respectively, and $I_t^H(p)$ and $B_t^H(p)$ denote their corresponding hue values, respectively. As observed from experiments, the differences in values of saturation and hue between the current frame and its background are often not large, which is consistent with the results reported in the work [15]; therefore, the values of τ_s and τ_H in this work are

taken as 0.6 and 70, respectively. The shadow points (in green) detected by the proposed algorithm are shown in Fig. 2(b)

The detection of car headlights is inspired and modified from our previous work [17]. In rainy conditions, drivers normally turn on their headlights to illuminate the ground. These relatively lighter regions are often misclassified as a moving object during background subtraction. Therefore, ground illumination should be removed to increase the accuracy of object segmentation, and thus improve the performance of subsequent tracking and classification. The detection of car headlights is proposed as.

$$L_t(p) = \begin{cases} 1, & \text{if } ((I_t^V(p) > \beta_1) \text{ and } (I_t^R(p) > \beta_2 \text{ and } I_t^G(p) > \beta_2 \text{ and } I_t^B(p) > \beta_2)) \\ 0, & \text{otherwise} \end{cases} \quad (3)$$

where $L_t(p) = 1$ denotes that the point $p(x, y)$ at the current frame belongs to the ground illumination of a car headlight, and $I_t^V(p)$ and $I_t^X(p)$, $\chi \in \{R, G, B\}$, represent the gray intensity and R, G, B channels of a given point $p(x, y)$, respectively. The rule in Eq. (3) is built based on the observation that points in an illuminated area have a higher gray intensity than a given threshold. The results of detected headlight points (in red) are shown in Fig. 2(d).

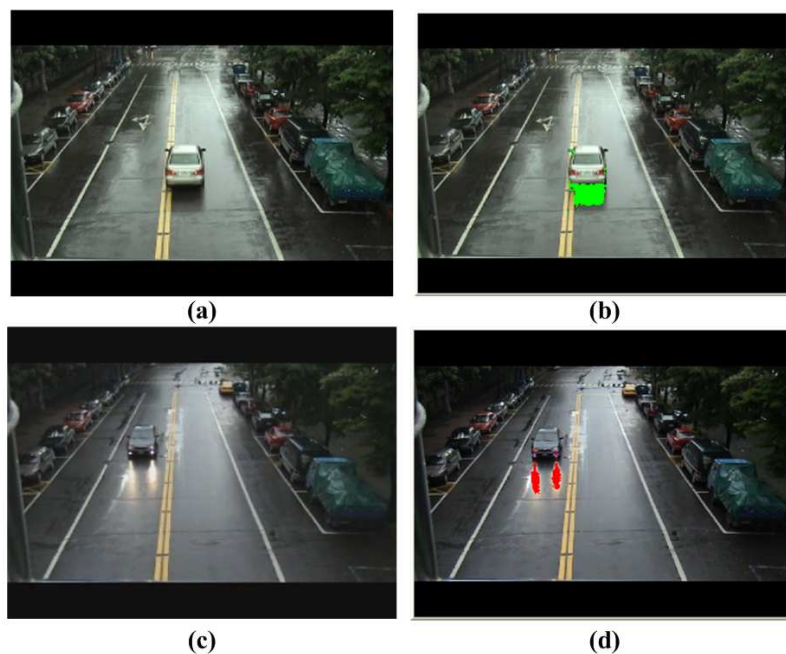


FIGURE 2. Results of the detection of shadows and headlight illumination. (a and c) Original images, (b) result of detected shadows (green), and (d) result of detected headlight illumination (red).

2.2. Removal of raindrops. In rainy situations, raindrops are often erroneously detected as moving objects during background subtraction, and thus greatly affect the reliability of subsequent object tracking and classification. The method of raindrop filtering was presented in our previous work [14]. Raindrops have three discernible features: a gray intensity feature, an appearance feature, and a temporal feature. Thus, moving objects with the three features are recognized as raindrops. (1) Gray intensity: raindrops have a higher gray intensity than those of the corresponding pixels in the background. (2) Appearance: raindrops appear as either a particle or a long strip. (3) Temporal: raindrops

in consecutive frames do not overlap if the frame rate used is higher than 30. Here, we briefly describe this method as follows.

To identify the gray intensity feature of raindrops, the total numbers of pixels in the k th foreground object in the frames of DF and DPF, $N_k(DF)$ and $N_k(DPF)$, are calculated, respectively, where DF means the difference frame that is obtained by subtracting the background from the original image, and DPF represents the difference positive frame that is obtained from the DF but only keeping the pixels with higher gray intensity in the original image than that in the background. Therefore, the criterion given in Eq. (4) is proposed to determine whether a moving object meets the condition of the gray intensity feature of raindrops.

$$T_1 = \begin{cases} 1, & N_k(DPF)/N_k(DF) \geq Tr_1 \\ 0, & otherwise \end{cases} \quad (4)$$

In theory, the ratio of these two values should be close to 1; however, Tr_1 is chosen as 0.90 here to allow for some image noise. A raindrop appears as either a particle or a long strip. Particle-shaped raindrops can be easily removed using morphological operations and noise filtering due to their small size; however, longstrip raindrops cannot be readily filtered out due to their relatively large size. To remove long-strip raindrops, the aspect ratio (height/width) of the raindrop is used to determine whether a detected moving object meets the requirement of the appearance feature of raindrops. Therefore, long-strip raindrops can be filtered out using the criterion given in Eq. (5).

$$T_2 = \begin{cases} 1, & Hr/Wr > Tr_2 \text{ AND } Wr \leq Tw \\ 0, & otherwise \end{cases} \quad (5)$$

where Hr and Wr are the height and width of the raindrop, respectively, and Tr_2 is a predetermined threshold set to 5. However, since the shapes of scooters or motorcycles meet the condition of $Hr/Wr > Tr_2$, another criterion, $Wr \leq Tw$ is required to avoid recognizing them as a longstrip raindrop.

To identify the temporal feature of raindrops, the ratio of a moving object overlapped in successive frames is used to determine whether it is a raindrop. Let $p_k^t(m)$ be the m th pixel of the k th moving object in the t th frame and $Np_k^t(m) = 1$ denote that pixel $p_k^t(m)$ in the current frame is overlapped by pixel $p_k^{t-1}(m)$ in the previous frame. Thus, the raindrops of the k th moving object with the temporal correlation in successive frames can be removed using the criterion given in Eq. (6).

$$T_3 = \begin{cases} 1, & \text{if } No_k/N_k < Tr_3 \\ 0, & otherwise \end{cases}, \text{ where } No_k = \sum_{m=0}^{N_k-1} Np_k^t(m) \quad (6)$$

where N_k is the total number of pixels in the k th moving object, No_k is the number of pixels in the current frame that overlap the pixels in the previous frame, and $Tr_3 \in [0, 1]$ is a threshold set to 0.1, which is reasonable for raindrops with only a small fraction of overlap.

The matching scores obtained using the gray intensity feature, the appearance feature, and the temporal feature, are then combined to identify whether the detected moving objects are raindrops.

$$T_{RN} = \begin{cases} 1, & \text{if } (T_1 = 1 \text{ and } T_2 = 1) \text{ or } (T_3 = 1) \\ 0, & otherwise \end{cases} \quad (7)$$

In the test video sequences, most of the moving objects such as cars and bikes do not meet the requirement of the temporal feature of raindrops; hence, this criterion ($T_3 = 1$) is

logically ORed with the other two criteria ($T_1 = 1$ and $T_2 = 1$). In our case, if accumulated raindrops in a time period are greater than a specified threshold, the weather is considered as rainy; at that time, the module of raindrop removal is initialized. The result of moving object detection after raindrop removal is shown in Fig. 3.

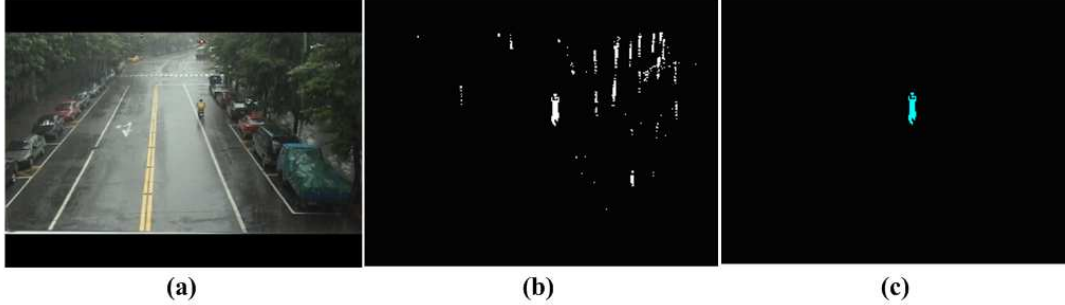


FIGURE 3. Result of moving object detection after raindrop removal. (a) Original image; (b) result of foreground detection; (c) result of moving object detection after raindrop removal.

2.3. Feature extraction and vehicle tracking. Numerous features, such as texture, color, and shape, are often used to detect a moving target. These features can be roughly classified as spatial features or temporal features. Spatial features are often used to discriminate objects at a given time, and temporal features are used for recognizing an object at different points in time. To recognize objects, specific features that can discriminate between various moving objects must be selected.

For a moving vehicle, features such as perimeter and area may vary with time due to vehicle approaching or moving away from the video camera. To reduce the effect of feature variation, an analysis of the bounding box of a moving object is introduced [18]. The aspect ratio, which only slightly varies with motion, is used for the tracking of moving objects. The vehicle aspect ratio, ζ , is defined as:

$$\zeta = \frac{Height}{Width} \quad (8)$$

where *Height* and *Width* are the height and width of the bounding box, respectively. For vehicle tracking and counting, the centroid of each moving object is calculated as follows.

$$x_c = \frac{\sum_{(x,y) \in R} x}{\sum_{(x,y) \in R} 1}, \quad y_c = \frac{\sum_{(x,y) \in R} y}{\sum_{(x,y) \in R} 1} \quad (9)$$

where (x_c, y_c) is the centroid of a moving object, and R is the set of pixels of the moving object.

Figure 4 shows the distribution of aspect ratio for cars (including buses and trucks) using 375 samples and bikes using 431 samples in several video sequences, respectively. The mean aspect ratios and their standard deviations were 1.47 and 0.14 for cars, and 2.15 and 0.25 for bikes, respectively. Therefore, vehicle classification can be achieved using the aspect ratio. As for the vehicle tracking algorithm, it is clearly described in our previous work [19].

The proposed method has some limitations. (1) When the area of a moving object is smaller than a prescribed threshold, the object is regarded as noise, and is thus removed

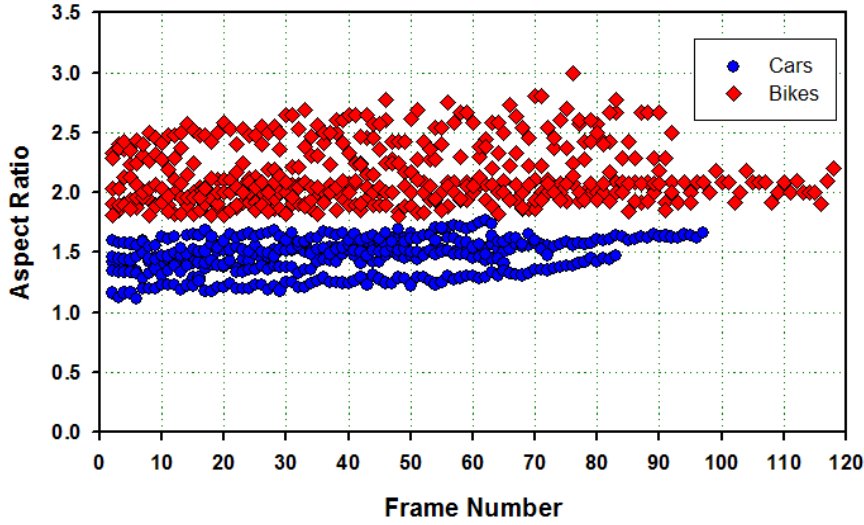


FIGURE 4. Distribution of aspect ratios for cars (375 samples) and bikes (431 samples).

from the template list. (2) When two moving objects intersect, they are detected as a single object, and one of them is removed from the template list; this problem can be overcome by using the color vector, as described in our previous study [20]. (3) When the moving object is split into two or more objects, each new moving object is added to the template list and counted if it reaches the virtual baseline; this problem has been solved in our previous study [20].

In order to achieve vehicle counting in a traffic surveillance system, the proposed method tracks each moving object between successive image frames. After segmentation of moving targets, objects and their bounding boxes and centroids are extracted from each frame. Two moving objects that are spatially closest in consecutive frames are correlated. The Euclidean distance is suitable to measure the distance between their centroids. The aspect ratio of vehicles, ζ , is considered to improve the tracking performance of moving objects. For each moving object in the current frame, an object with the minimum distance of centroids and the closest value of aspect ratio between two consecutive frames is considered to be the same one in the previous frame. The criteria for object matching are given in Eqs. (10) and (11), respectively.

$$|\zeta_t^m - \zeta_{t-1}^n| < \zeta_{Th} \quad (10)$$

$$dist(ctd_t^m, ctd_{t-1}^n) = \sqrt{(xc_t^m - xc_{t-1}^n)^2 + (yc_t^m - yc_{t-1}^n)^2} < \delta_{Th} \quad (11)$$

where m and n are the indices of each moving object, t and $t - 1$ denote the current and previous frames, respectively, ctd represents the centroid of each moving, and ζ_{Th} and δ_{Th} are thresholds that are determined from experimental observations, where ζ_{Th} is set to one standard deviation of the aspect ratios of cars and bikes, respectively. However, if $dist$ is the minimum between the m th object in the t frame and the n th object in the $t - 1$ frame, and the criterion of $dist < \delta_{Th}$ is satisfied, the moving object in the current frame is tracked.

2.4. Vehicle classification. To overcome the problem of using only one reference frame [18, 21], the proposed method extracts the aspect ratio from consecutive frames to achieve a

robust and highly accurate classification of moving vehicles. Two accumulators, namely *Acc_Car* and *Acc_Bike*, are used to sum the features extracted from a given car or bike in the test videos, respectively. If the extracted feature is regarded as belonging to a car, the accumulator of *Acc_Car* is increased by one; otherwise, the accumulator of *Acc_Bike* is increased by one. After a period of time, the values of *Acc_Car* and *Acc_Bike* are used to determine the type of vehicle. Figure 5 shows a flowchart of the proposed method for vehicle classification. The value of the threshold is set from experiments. The results of vehicle classification in various situations are shown in Fig. 6, where green and blue bounding boxes are used for bikes and cars, respectively.

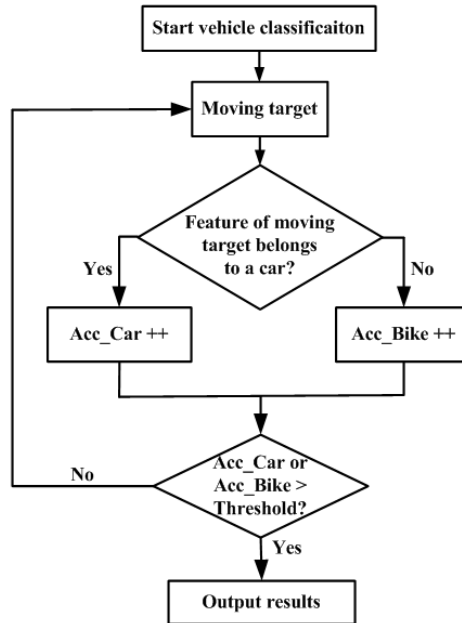


FIGURE 5. Flowchart of proposed method for vehicle classification based on aspect ratio.

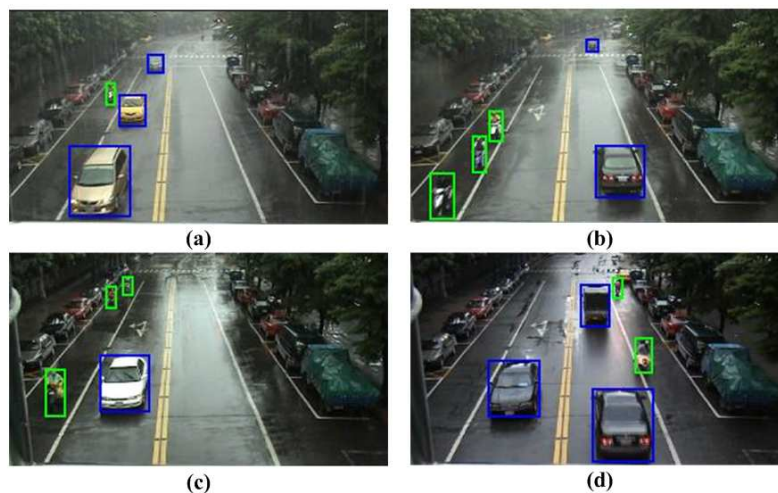


FIGURE 6. Results of vehicle classification of bikes (green boxes) and cars (blue boxes).

3. Experimental Results. To evaluate the performance of the proposed scheme for vehicle flow measurement, six videos in rainy conditions captured for city roads and highways, respectively, were used. In the test videos, CityRoad_01 has 8400 frames, CityRoad_02 has 7170 frames, CityRoad_03 has 6300 frames, Highway_01 has 1980 frames, Highway_02 has 1380 frames, and Highway_03 has 1950 frames. Note that the first three videos were captured for the same road under different rain conditions, and the last three videos were downloaded from a website (<http://1968.nfreeway.gov.tw>) maintained by the National Freeway Bureau in Taiwan. In these cases, the traffic conditions of the city road for each image from the video sequence were quite similar over a long time; therefore, several-minute clips of the test videos were sufficient to evaluate the performance of the proposed method. The video has a resolution of 320×240 pixels and is captured at a frame rate of 30 fps.

The proposal of raindrop filtering module eliminates the interference of raindrops, which greatly enhances the performance of vehicle tracking and subsequent classification. To verify the performance of the proposed raindrop filtering module, the measure of spatial accuracy [22], as defined in Eq. (12), is suitable. It is often used to evaluate the performance of moving object segmentation. In Eq. (12), $M_n^{ref}(x, y)$ represents the mask of the ground truth at frame n , $M_n^{seg}(x, y)$ is the mask of the resulting segmentation of moving objects by the proposed method, and \oplus denotes the logical exclusive OR operation. This measure can be used to estimate the distortion between the masks of the ground truth and the segmentation of moving objects obtained using the proposed method. In Eq. (12), the second term inside parentheses is employed to calculate the fraction of wrongly recognized pixels of moving objects as background ones.

$$Spatial\ accuracy = \left(1 - \frac{\sum_{(x,y)} M_n^{ref}(x, y) \oplus M_n^{seg}(x, y)}{\sum_{(x,y)} M_n^{ref}(x, y)} \right) \times 100\% \quad (12)$$

The results of spatial accuracy for the three test videos of a city road are shown in Fig. 7, where F_n is the current frame number, F_0 is the first frame number with moving objects, and F_e is the last frame number with moving objects. For the three cases in rainy conditions, the average values of spatial accuracy without the aid of raindrop filtering are 53.52%, 60.50%, and 61.89% for the test videos of CityRoad_01, CityRoad_02, and CityRoad_03, respectively. With raindrop filtering, the average spatial accuracies increase to 74.37%, 67.66%, and 74.55%, respectively. Therefore, raindrop filtering greatly improves the segmentation of moving objects.

In order to analyze the vehicle flow, the configuration shown in Fig. 8 was adopted. A color video camera was installed about 5m above road level on the central lane of the road, facing the road traffic at an angle of 65° . To achieve bidirectional counting of vehicles, baselines 1 and 2 (virtual lines) were used. These two baselines indicate the locations at which the system counts the moving vehicles. The baselines were set according to the distance between the camera and the road. The counting procedure was initiated when moving vehicles passed through area R2 to baseline 1 or baseline 2, depending on the movement direction of vehicles. The results of vehicle counting for six test videos are shown in Fig. 9. White, blue, and green boxes indicate an undetermined vehicle type, cars, and bikes, respectively.

The geometric features of area ratio and compactness were also evaluated for vehicle classification, which are defined as $Area/ROI$ and $Perimeter^2/Area$, respectively, where $Area$ and $Perimeter$ denote the area and corresponding perimeter of a moving object, respectively, and ROI is the area of the bounding box of a moving object. In this

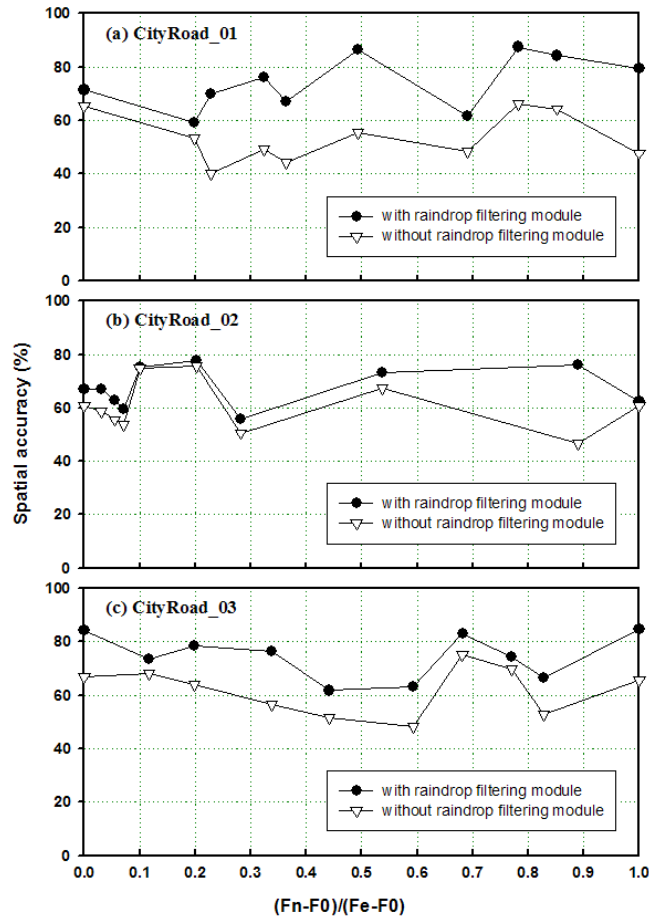


FIGURE 7. Spatial accuracy of object segmentation for the three test videos with and without the aid of raindrop filtering module. (a) CityRoad_01, (b) CityRoad_02, and (c) CityRoad_03.

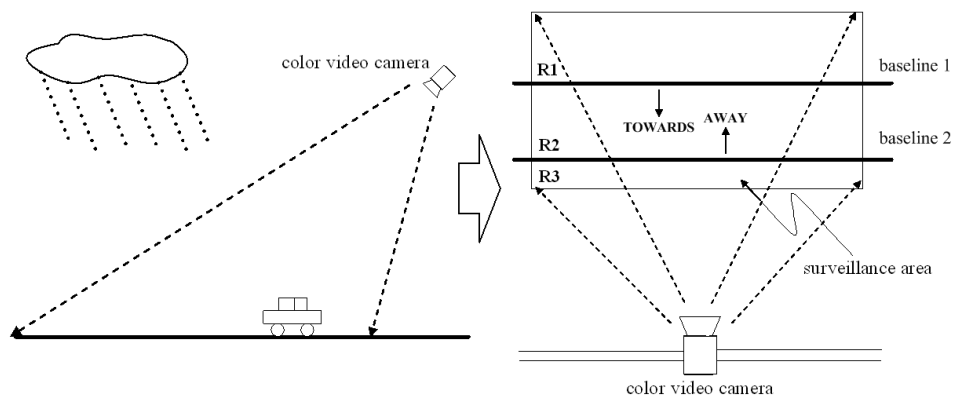


FIGURE 8. Configuration of color video camera for proposed vehicle counting system.

experiment, 317 vehicle samples, including 138 cars and 179 bikes, in the collected video sequences were used. Table 1 shows the effect of the feature type on the performance of vehicle classification. For the test video sequence, the proposed system tracked and classified most cars successfully using the features of aspect ratio and area ratio. The best

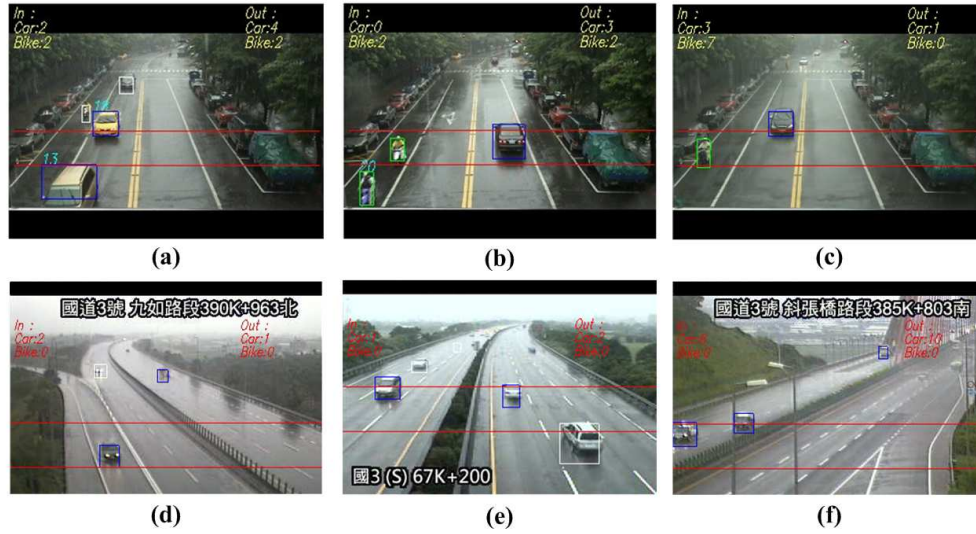


FIGURE 9. Results of vehicle counting for six test videos. Images taken from (a) CityRoad_01, (b) CityRoad_02, (c) CityRoad_03, (d) Highway_01, (e) Highway_02, and (f) Highway_03.

classification rates for cars (96.4%) and bikes (92.7%), respectively, were obtained using the feature of aspect ratio. The aspect ratio was thus used for vehicle classification in this work.

TABLE 1. Confusion matrix illustrating the effect of feature type on the performance of vehicle classification

	Aspect ratio		Area ratio		Compactness	
	Car	Bike	Car	Bike	Car	Bike
Car	133 (96.4%)	5 (3.6%)	129 (93.5%)	9 (6.5%)	106 (76.8%)	32 (23.2%)
Bike	13 (7.3%)	166 (92.7%)	66 (36.9%)	113 (63.1%)	58 (32.4%)	121 (67.6%)

TABLE 2. Vehicle counting accuracy for test videos of a city road

	Number of vehicles		Number of correctly recognized vehicles		Recognition rate	
	Car	Bike	Car	Bike	Car	Bike
CityRoad_01	18	16	16	14	88.9%	87.5%
CityRoad_02	24	18	21	15	87.5%	83.3%
CityRoad_03	17	19	15	16	88.2%	84.2%
Total	59	53	52	45	88.1%	84.9%

For highway evaluation, only cars were counted since other types of vehicles are not permitted on highways in Taiwan. For the city road, the average vehicle counting accuracies were 88.1% and 84.9% for cars and bikes, respectively (see Table 2). However, for the highway, the average car counting accuracies for the directions of TOWARDS and AWAY were 86.9% and 96.3%, respectively (see Table 3). The segmentation accuracy of

moving objects greatly affects the performance of vehicle tracking and subsequent classification. Factors such as weather conditions, light conditions, and shadows and headlights of vehicles greatly impact the performance of object segmentation. Hence, it is quite difficult to achieve highly accurate vehicle counting under all traffic conditions. However, the proposed method achieved average recognition rates of greater than 86.9% and 84.9% for cars and bikes, respectively.

TABLE 3. Car counting accuracy for test videos of a highway

	Number of cars		Number of correctly recognized cars		Recognition rate	
	TO-WARDS	AWAY	TO-WARDS	AWAY	TO-WARDS	AWAY
Highway_01	17	16	16	15	94.1%	93.8%
Highway_02	30	23	25	22	83.3%	95.7%
Highway_03	14	15	12	15	85.7%	100.0%
Total	61	52	53	54	86.9%	96.3%

4. Conclusion. A feature-based vehicle counting method that performs well in rainy conditions was proposed. The method integrates the subsystems of background subtraction, the removal of shadows and headlights, raindrop filtering, and vehicle tracking and classification. The background pixels are determined based on the selection of the most likelihood of gray intensities for each point. The feature of aspect ratio is used in the proposed method to improve the performance of vehicle classification. The raindrop filtering module eliminates the interference from raindrops in the segmentation of moving objects. The average spatial accuracies were greatly improved from 53.52%, 60.50%, and 61.89% to 74.37%, 67.66%, and 74.55% for the videos CityRoad_01, CityRoad_02, and CityRoad_03, respectively, with the aid of raindrop filtering. For a city road, the average vehicle counting accuracies were 88.1% and 84.9% for cars and bikes, respectively. For a highway, the average car counting accuracies for the lane directions of TOWARDS and AWAY were 86.9% and 96.3%, respectively. The results of vehicle counting show the feasibility of the proposed method under rainy conditions.

Acknowledgment. This work is partially supported by National Science Council under Grant NSC96-2622-E-151-016-CC3 and Ministry of Education under Grant 97E-05-172, Taiwan, R.O.C.

REFERENCES

- [1] C. R. Wren, A. Azarbayejani, T. Darrell, A. P. Pentland, Pfinder: real-time tracking of human body, *IEEE Transactions on Pattern Analysis and Machine Intelligence*, vol. 19, no.7, pp. 780-785, 1997.
- [2] C. Stauffer, and W. Grimson, Adaptive Background Mixture Models for Real-Time Tracking, *Proc. IEEE Conference on Computer Vision and Pattern Recognition*, Fort Collins, Colorado, USA, pp. 246-252, 1999.
- [3] N. A. Mandellos, I. Keramitsoglou, and C. T. Kiranoudis, A background subtraction algorithm for detecting and tracking vehicles, *Expert Systems with Applications*, vol. 38, no.3, pp. 1619-1631, 2011.
- [4] B. Zhang, B. Zhong, and Y. Cao, Complex background modeling based on texture pattern flow with adaptive threshold propagation, *Journal of Visual Communication and Image Representation*, **22**(6), pp. 516-521, 2011.
- [5] S. McKenna, S. Jabri, Z. Duric, A. Rosenfeld, and H. Wechsler, Tracking Groups of People, *Computer Vision and Image Understanding*, vol. 80, no. 1, pp. 42-56, 2000.

- [6] A. Mohan, C. Papageorgiou, and T. Poggio, Example-Based Object Detection in Images by Components, *IEEE Transactions on Pattern Analysis and Machine Intelligence*, vol. 23, no. 4, pp. 349-361, 2001.
- [7] T. J. Fan, G. Medioni, and G. Nevatia, Recognizing 3-D Objects Using Surface Descriptions, *IEEE Transactions on Pattern Analysis and Machine Intelligence*, vol. 11, no. 11, pp. 1140-1157, 1989.
- [8] B. Schiele, Model-Free Tracking of Cars and People Based on Color Regions, *Proc. IEEE International Workshop on Performance Evaluation of Tracking and Surveillance*, Grenoble, France, pp. 61-71, 2000.
- [9] L. Huang, Real-Time multi-vehicle detection and sub-feature based tracking for traffic surveillance systems, *Proc. of IEEE International Asia Conference on Informatics in Control, Automation and Robotics*, Wuhan, China, 2010.
- [10] W. Hu, T. Tan, L. Wang, and S. Maybank, A Survey on Visual Surveillance of Object Motion and Behavior, *IEEE Transactions on Systems, Man, and Cybernetics—Part C: Applications and Reviews*, vol. 34, no. 3, pp. 334-352, 2004.
- [11] K. Garg, and S. K. Nayar, Detection and removal of rain from videos, *Proc. of IEEE Computer Society Conference on Computer Vision and Pattern Recognition*, Washington, DC, USA, 2004.
- [12] S. Gormer, A. Kummert, P. Su-Birm, and P. Egbert, Vision-based rain sensing with an in-vehicle camera, *Proc. of IEEE International Symposium on Intelligent Vehicles*, Xian China, 2009.
- [13] A. Cord, and D. Aubert, Towards rain detection through use of in-vehicle multipurpose cameras, *Proc. of IEEE International Symposium on Intelligent Vehicles*, Baden-Baden, Germany, 2011.
- [14] D. Y. Huang, C. H. Chen, W. C. Hu, and S. S. Su, Reliable moving vehicle detection based on the filtering of swinging tree leaves and raindrops, *Journal of Visual Communication and Image Representation*, vol. 23, no. 4, pp. 648-664, 2012.
- [15] R. Cucchiara, C. Grana, M. Piccardi, and A. Prati, Detecting moving objects, ghosts, and shadows in video stream, *IEEE Transactions on Pattern Analysis and Machine Intelligence*, vol. 25, no. 10, pp. 1337-1342, 2003.
- [16] A. Prati, I. Mikic, M. M. Trivedi, and R. Cucchiara, Detecting moving shadows: Algorithms and evaluation, *IEEE Transactions on Pattern Analysis and Machine Intelligence*, vol. 25, no. 7, pp. 918-923, 2003.
- [17] T. H. Chen, J. L. Chen, C. H. Chen, and C. M. Chang, Vehicle detection and counting by using headlight information in the dark environment, *Proc. of IEEE International Conference on Intelligent Information Hiding and Multimedia Signal Processing*, Kaohsiung, Taiwan, 2007.
- [18] L. Bo and Z. Heqin, Using object classification to improve urban traffic monitoring system, *Proc. IEEE International Conference on Neural Networks and Signal Processing*, Toulouse, France, pp.1155-1159, 2003.
- [19] D.Y. Huang, C.H. Chen, W.C. Hu, S.C., and Y.F. Lin, Feature-based vehicle flow analysis and measurement for a real-time traffic surveillance system, *Journal of Information Hiding and Multimedia Signal Processing*, vol. 3, no. 3, pp. 282-296, 2012.
- [20] C. H. Chen, T. Y. Chen, D. J. Wang, and T. J. Chen, A Cost-Effective People-Counter for a Crowd of Moving People Based on Two-Stage Segmentation, *Journal of Information Hiding and Multimedia Signal Processing*, vol. 3, no. 1, pp. 12-25, 2012.
- [21] B. L. Tseng, C. Y. Lin, and J. R. Smith, Real-Time Video Surveillance for Traffic Monitoring Using Virtual Line Analysis, *Proc. IEEE International Conference on Multimedia and Expo*, Lausanne, Switzerland, pp.541-544, 2002.
- [22] T. Y. Chen, C. H. Chen, D. J. Wang, and Y. C. Chiou, Real-Time Video Object Segmentation Algorithm Based on Change Detection and Background Updating, *International Journal of Innovative Computing, Information and Control*, vol. 5, no.7, pp. 1797-1810, July 2009.